

## Stimulus Dependent Neural Correlations in the Auditory Midbrain of the Grassfrog (*Rana temporaria* L.)

I. J. Eggermont, W. J. M. Epping, and A. M. H. J. Aertsen

Department of Medical Physics and Biophysics, University of Nijmegen, Nijmegen, The Netherlands

**Abstract.** Few-unit recordings were obtained using metal microelectrodes. Separation into single-unit spike trains was based on differences in spike amplitude and spike waveform. For that purpose a hardware microprocessor based spike waveform analyser was designed and built. Spikes are filtered by four matched filters and filter outputs at the moments of spike occurrence are read by a computer and used for off-line separation and spike waveform reconstruction. Thirty-one double unit recordings were obtained and correlation between the separated spike trains was determined. After stimulus correction correlation remained in only 8 of the double unit records. It appeared that in most cases this neural correlation was stimulus dependent. Continuous noise stimulation resulted in the strongest neural correlation remaining after correction for stimulus coupling, stimulation with 48 ms duration tonepips presented once per second generally did not result in a significant neural correlation after the correction procedure for stimulus lock. The usefulness of the additive model for neural correlation and the correction procedure based thereupon is discussed.

### Introduction

A wealth of knowledge about the auditory nervous system has resulted from single unit studies performed in nearly all levels in the brain: from auditory nerve to auditory cortex. When using single unit data to gain insight in the auditory system or part thereof, one implicitly assumes that a sufficiently large sample of neural units covers the properties of a particular nucleus. One thereby discovers that neural properties become more and more complex when advancing to higher levels in the nervous system. For the auditory nerve the frequency response curves (tuning curves)

and latency or PST histograms (Kiang et al., 1965) provide the bulk of information that is needed to characterize the neuron, and together with suppression regions and rate-intensity functions give a fairly complete impression about the properties of the nerve. At higher levels in the CNS highly specialized units have been found, e.g. velocity-coding neurons in the bat cortex but relatively simple neural networks can account for these properties (Suga, 1973). The neurons are no longer characterised by simple measures as tuning or latency and rate-function independently.

In contrast multi-unit studies are mainly used to arrive at an overall idea about the functioning of the system (e.g. Brzoska et al., 1977; Lombard et al., 1981) and seem to perform well in estimating hearing threshold as a function of frequency or in areas with an orderly representation of the stimulus parameter under study. For supraliminal use the disadvantage is that those neurons with a high firing rate dominate the obtained result completely, as is probably also the case in the deoxyglucose labeling technique (paton et al., 1982).

An intermediate situation is obtained when only a few units are recorded simultaneously and one is able to recognize and separate the individual neuron's contributions. In the current exploration of the nervous system one considers a spike as an event i.e. one assumes the actionpotential waveform to be irrelevant. Only a few studies on the auditory nervous system have explicitly dealt with the functional significance of spike waveform (pfeiffer, 1966; Robertson, 1976; Eggermont et al., 1981). In contrast quite a few investigations studying neural interaction use differences in spike waveforms to separate multi-unit spike trains into single unit spike trains (e.g. Abeles and Goldstein, 1977).

In recent years it has been found that neurons within the auditory nerve of the cat are functionally uncorrelated (Johnson and Kiang, 1976) and that

inhibitory interactions exist between type II/III and type IV cells in the dorsal cochlear nucleus of the cat (Voigt and Young, 1980) as was suggested from morphological studies (Osen, 1969). It was furthermore observed that in pairs of units recorded with one electrode from the rabbit inferior colliculus best frequency was always identical (Syka et al., 1981), a consequence of the highly organized structure of this nucleus. For the medial geniculate body in the cat it was found that up to 40 % of the units showed some type of neural interaction, that in addition up to 20 % of the neuron pairs studied had common input, but that there was a surprisingly small number of neurons that showed inhibitory interactions (Heierli et al., 1981). Simultaneous recordings of neurons in the MGB and primary auditory cortex of the guinea pig showed that in 9 out of 69 pairs investigated a positive correlation with a 2-5 ms delay was found, indicating a monosynaptic excitatory influence (Creutzfeldt et al., 1980). Finally for auditory units in the cortex of the cat in 22 out of 30 pairs recorded with a single electrode strong neural coordination was observed, while only 6 out of 37 pairs recorded with mechanically independent but closely spaced electrodes showed this (Dickson and Gerstein, 1974).

In the list of citations we have used the words correlation, interaction and coordination as the respective authors did. We have the feeling that some more general rule for the use of these words must be formulated. As coordination is a rather functional description of an active process we suggest to drop the use of this word entirely. For the various manifestations of neural interaction (the mechanism underlying a significant correlation between spike trains under non-stimulus conditions and excluding common input) we propose the following hierarchical structure: neural synchrony, neural correlation and neural interaction. Neural synchrony is the manifestation of a correlation between spike trains irrespective of stimulus conditions. Neural correlation is the significant correlation between spike trains under stimulus conditions that remains after a stimulus correction procedure (e.g. Perkel et al., 1967) and including the common input situation under non-stimulus conditions. Neural interaction is then defined as above.

Animal behavior is strongly context dependent even in amphibians (Ewert et al., 1982). Considering the underlying neural activity to be the basis of this dependency one may ask whether neural interaction is due to a hard-wired unchangeable lay-out or that either the type or the strength of the neural interaction may change under differing stimulus conditions.

In the central nervous system single unit activity differs under different stimulus conditions. For instance, in the torus semicircularis of the grassfrog the

spectro temporal sensitivity (STS) to single tones can be different from that obtained for stimulation with natural sounds (e.g. Aertsen and Johannesma, 1980) or from that obtained using gaussian noise stimulation (Hermes et al., 1981, 1982). This can possibly be explained by invoking that the neuron functions within a neural net and that the interaction between the neurons involved is stimulus dependent.

The present paper aims to outline the procedures used for the study of neural interaction in the torus semicircularis in the grassfrog, to emphasize the use of a wide ensemble of different stimuli to study this proposed stimulus dependence, and to provide evidence for the existence of stimulus dependent neural correlation.

## Methods

### 1 Preparation

Under MS-222 anaesthesia the optic tectum of the grassfrog was exposed (details in Hermes et al., 1981) and the frog was allowed to recover for two days. Local anaesthetic was then applied to the exposed tissue and the animal was immobilized with an intralymphatic injection of Buscopan. The ECG was monitored using a right fore leg - left hind leg recording and served as a measure for pain or arousal of the animal during the experiments. The heart rate was very constant and slightly dependent on temperature and state of the paralysis. At 16°C the rate usually was between 30 and 40 per min. Any pain deliberately induced caused the ECG to increase in rate by up to 10 %, the same effect but smaller was found when stimulating the animal with 89 dB RMS wide band noise. These effects were absent if the animal was anaesthetized with MS-222. We interpreted constancy of the ECG therefore as an indication that pain nor arousal were present. For each stimulus presentation the average heart rate was calculated by computer and displayed. Temperature was kept constant ( $\pm 10$ C) around 16°C, a temperature at which oxygen exchange through the skin is sufficient for metabolic demands.

### 2 Few Unit Recording

Metal (stainless steel or tungsten) electrodes with an exposed tip of about 10  $\mu$ m and a 1 kHz impedance in the 1-3 M $\Omega$  range are suited to obtain double or triple unit recordings. Cell diameter appears to be correlated to spike amplitude for brainstem nuclei in the cat (Grover and Buchwald, 1970) in multi unit recording. One expects more or less the same effect in few unit recordings: a population of cells of inhomogeneous size will give rise to spikes of different amplitude. Another factor of importance is the distance, R, be-

tween electrode and nerve cell. The voltage recorded is expected to decrease with distance as  $R^{-1}$  for a point source (cell body) or as  $R^{-2}$  for a dipole (axon). Still another important factor arises from the specific geometry of the recording electrode cell configuration. It is therefore expected that in general the activity recorded by one and the same electrode from two or three units will be distinguishable on basis of waveform and amplitude differences.

In the present experiments we used commercially obtained ultra-fine tapered tungsten or stainless steel electrodes coated with parylene-c having a 10-15/μm exposed tip with a 1kHz impedance of about 1.5-2 MΩ (BAK electronics Inc). The electrodes were advanced through the exposed dura and lowered into the auditory midbrain using a motorised hydraulic micro drive (Trent-Wells, 3-0661). The electrode signal was amplified using a DAGAN extracellular pre-amplifier band passed between 100 Hz and 10 kHz.

### 3 Separation of Few-Unit Spike Trains

For few-unit recordings made with one single electrode a number of separation schemes have been developed, all using features derived from the spike waveform. It is thereby assumed that the spike waveform is characteristic for a particular neuron in a given geometric position to the recording electrode. The feature extraction procedures can be parametric procedures using a priori selected features such as amplitude, time between zero crossings, slope of waveform segments etc. (e.g. Vibert and Costa, 1979; Dinning and Sanderson, 1981). These methods allow generally a good separation tailored to a particular situation but do not permit off-line reconstruction of separated waveforms. The second group of schemes uses the entire spike waveform and applies a generalized distance to a selected waveform as a separation measure (e.g. Gerstein, 1970; D'Hollander and Orban, 1979) or uses a matched filter approach (e.g. Glaser, 1971; Abeles and Goldstein, 1977). This last method allows an efficient description of the entire spike waveform using only a few parameters which are then used for storage, off-line reconstruction as well as separation of few unit spike trains. We have implemented a simple and convenient version of this method using a microprocessor based design, its basic elements and features will be described subsequently.

*a Spike Waveforms in the Frog's Brain.* On the basis of single unit recordings, using 2-14 MΩ stainless steel microelectrodes, in the torus semicircularis of *Rana temporaria* (Eggermont et al., 1981a) we arrived at five distinct types of waveforms (Fig. 1) Type I being a triphasic initially positive, low amplitude ( $< 150 \mu V$ ), fast spike, Type II representing a more low-frequency,

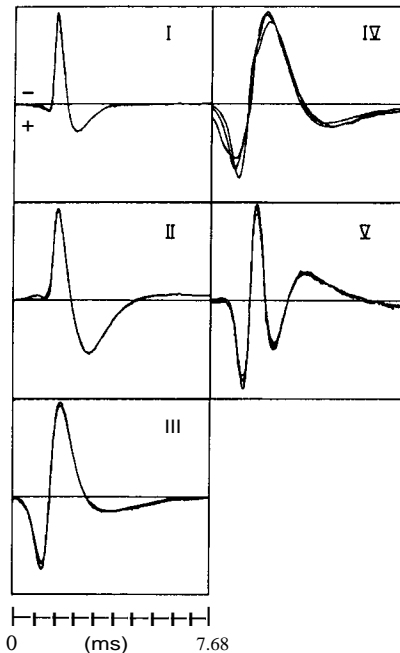


Fig. 1. Spike waveforms from the frog's brain. The three main types of spike waveforms recorded with metal microelectrodes are the types I, II and III. Occasionally the other types are observed. Type I is attributed to axons, type III is the most prominent one. Superimposed are reconstructions of spike waveforms based on four respectively eight basisvectors

biphasic negative-positive spike also of relatively low voltage ( $< 150 \mu V$ ), Types III, IV, V all starting with a large positive deflection and either bi-, tri- or polyphasic had larger voltage ( $> 300 \mu V$ ) and durations sometimes exceeding 5 ms. No correlation was found between spike waveform and recording electrode impedance, nor with particular animals. Correlations were, however, found with recording site as well as other neural properties suggesting a function associated with spike waveform (Eggermont et al., 1981b; Hermes et al., 1981). This multitude of waveform types has also been observed in the olfactory epithelium (Getchell, 1973) as well as in the optic tectum (Witpaard and Ter Keurs, 1975) of the frog; duration of the spike and voltage were in the same range. Also in these studies waveform was suggested to be functionally correlated with cell type or part of the cell recorded from.

*b Matched Filter Impulse Response.* In order to explore if sufficient information about the neurons is contained in the spike waveform and whether it can be represented by only a few parameters we have determined the necessary templates on the basis of a set of 64 average waveforms from as many single units. For recording temperatures of 15-18°C the spike waveforms never exceed a duration of 8 ms while in the powerspectra of the averaged waveforms little energy

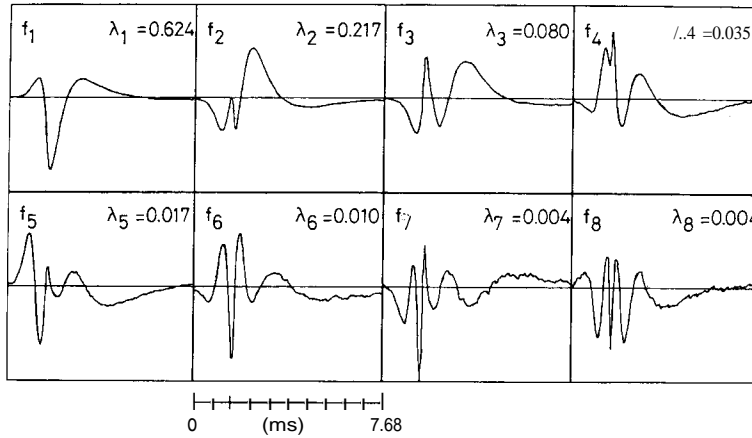


Fig. 2. Orthogonal templates for spike waveform decomposition. The indicated eigenvalues ( $\lambda_i$ ) represent the fraction of the energy in the population of spike waveforms that is represented by the particular template. One observes the initial rapid decrease and later stabilization in  $\lambda_i$  for increasing  $i$  ( $i=1, \dots, 8$ ). The first four templates represent about 95% of the energy in the spike waveforms, which was considered sufficient

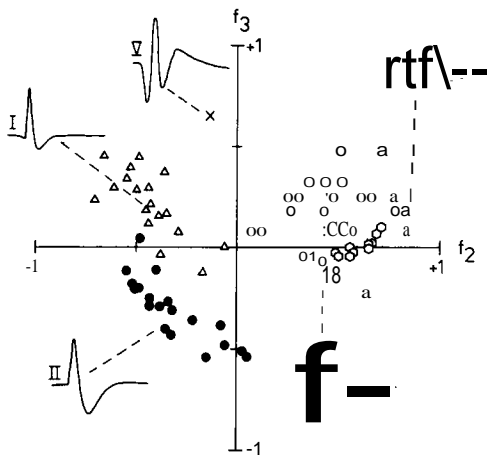


Fig. 3. Representation of the learning set of averaged spike waveforms on the  $f_2, f_3$  plane. All 64 waveforms used to construct the orthogonal templates are represented on the plane determined by the second- and third template. It appears that the a priori typification (cf. Fig. 1) leads to separable clusters and is thereby corroborated

was present above 8.5 kHz. Therefore the waveforms were sampled at a rate of 16.7 kHz with 128 samples (at 60  $\mu$ s per point this results in a total duration of 7.68 ms). The arbitrary start of each waveform was set at 1.5 ms before the detection moment of the spike determined by negative going level crossing on the negative polarity deflection. The templates (basis vectors) were calculated for the normalized spike waveforms (at equal energy) according to the Karhunen-Loeve expansion procedure (Fukunaga, 1972).

The eight basis vectors with largest eigenvalues (i.e. their ability to represent energy of the set of spike waveforms) are shown in Fig. 2. It is noted that the basisvectors become high frequent and noisy as the eigenvalues decrease. The first 4(8) basisvectors represent  $95.6 \pm 4.3\%$  ( $99.2 \pm 0.8\%$ ) of the energy contained in the set of waveforms. These values are comparable

to the 97.7% representation on 4 basisvectors derived by Abeles and Goldstein (1977) for the auditory cortex of the cat.

For optimal results in subsequent multi-unit experiments the *collection of waveforms* and therefore the collection of basisvectors must be *representative*. This has been investigated in three ways: first of all it was determined how 10 newly recorded single unit waveforms were represented by the present set of basisvectors. We found it to be as good as for the waveforms in the original set. Secondly, we investigated to what extent the basisvector space depended on the originating collection of waveforms. For this purpose the waveform set was divided, according to date of single unit recording, into two test sets each of 32 waveforms. For each test set basisvectors were computed. Besides a good resemblance of the two groups of basisvectors the 4(8) basisvectors from each set represented only  $2.3 \pm 2.4\%$  ( $0.63 \pm 0.64\%$ ) less of the energy from the "other" collection of waveforms than its own set of basisvectors did. The third way was simply to apply the separation procedure based on these basisvectors (determined over the complete set) to actual few unit recordings and to observe that quite good separation of individual waveforms was possible.

This is illustrated in Fig. 3 where the 64 individual averaged waveforms are projected onto the plane determined by the second and third basisvector. This indicates a good separation of the various waveform types, five of which are indicated by their waveforms, thereby corroborating the a priori made typology (Eggermont et al., 1981a and b). For the practical realisation we decided to use only the four most important basisvectors.

*c The Hardware Spike Waveform Analyzer.* The hardware spike analyzer consists of a level crossing spike detection unit, a spike waveform buffer memory, four in parallel operating matched filters, a timing unit, a

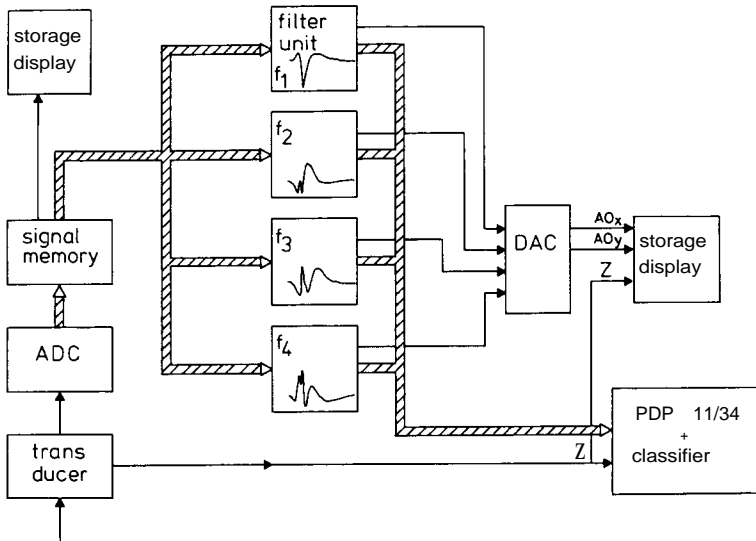


Fig. 4. Diagram of the hardware spike waveform analyzer. The basic features are 1. spikes are detected by level crossing; 2. the orthogonal templates are realised as digital, finite impulse response filters; 3. the output of the templates is sampled at the moment of level crossing (taking into account any filter delay); 4. the output values are displayed as in Fig. 3 for all template combinations; 5. moments of level crossing together with the output values of the matched filters are stored for off-line classification and spike waveform reconstruction

display and a connection to a PDP 11/34 computer (Fig. 4).

The matched filters are constructed as Finite Impulse Response digital filters, the impulse responses actually being the time-reversed basisvectors. The electrode signal passes continuously through the four filters and a running cross correlation between electrode signal and basis vectors is established. This correlation results every 60 IIS in four values (filter outputs) so that for each spike 128 "four-values" are available. Only one combination of "four-values" is important however: that particular set corresponding to the detection moment (event) of the spike. We will call this set the *label-set*. By taking into account the filter delay the output of the matched filters is only transferred to the computer as well as to the display unit when the event occurs. Simultaneously the spike waveform buffer memory containing the detected spike is read out and the spike waveform displayed, as well as the six possible combinations of two out of four labels are displayed in scattergrams. This latter approach serves to decide during the initial phase of the experiment if subsequent off-line separation of the clusters (cf. Fig. 5b) will be possible. The moment of spike detection (the event) is stored together with the four labels representing the spike waveform optimally. The spike analyzer was used with a dead time set at a-half template duration, i.e. 3.84ms. From the interval histograms it was clear that minimum spike intervals for single units were always longer.

*d Separation Procedure and Off-Line Reconstruction of Spike Waveforms.* Given the four basisvectors  $f_1, f_2, f_3$  and  $f_4$  and the labels  $a_1, a_2, a_3$  and  $a_4$  representing a spike, the original waveform is estimated by  $a = a_1 f_1 + a_2 f_2 + a_3 f_3 + a_4 f_4$  a vector in the four dimensional basisvector space. All spikes from a given neural unit

together will form a cluster in that space, different neural units will form different clusters (i.e. having different mean vectors  $J_{i_a}$  and  $J_{i_b}$ ) Good separation will be possible when the clusters do not overlap.

The separation procedure is done in an interactive way, it starts with the selection of that combination of two basisvectors (out of four) forming a plane on which the cluster projections appear best separable. Then an ellipse is constructed around one of the clusters by indicating with a cursor the end points of the long axis and one end point of the short axis. This ellipse can be seen as the "boundary" of the projection of a multivariate normal density function in the four dimensional space onto the plane determined by the two selected basisvectors.

Instead of each spike being characterised by a differing set of four labels all spikes within the separation ellipse now receive one new label: the number of the unit. All data points (representing spike waveforms) within the ellipse boundary are then considered to belong to one neuron, they are removed from the original multi-unit spike train. Then the procedure starts over again, optionally in another projection plane, a new ellipse is constructed around one of the remaining clusters etc. When all the spikes are classified (Fig. 5c) the original multi-unit dot display is separated into single unit dot displays (cf. Figs. 5d-f), and the spike waveforms belonging to a given class are superimposed and the average waveform is calculated. This superposition allows an inspection of the correctness of the separation procedure, and may indicate the necessity of a reclassification (Fig. 5g-i).

The set of  $\{a_i, i = 1, \dots, N, a_i = a_{i1}, \dots, a_{i28}\}$  forms the set of estimated spike waveforms for a given neural unit. The average waveform  $J_a^1 = \frac{1}{N} \sum_{i=1}^N a_i$  is a

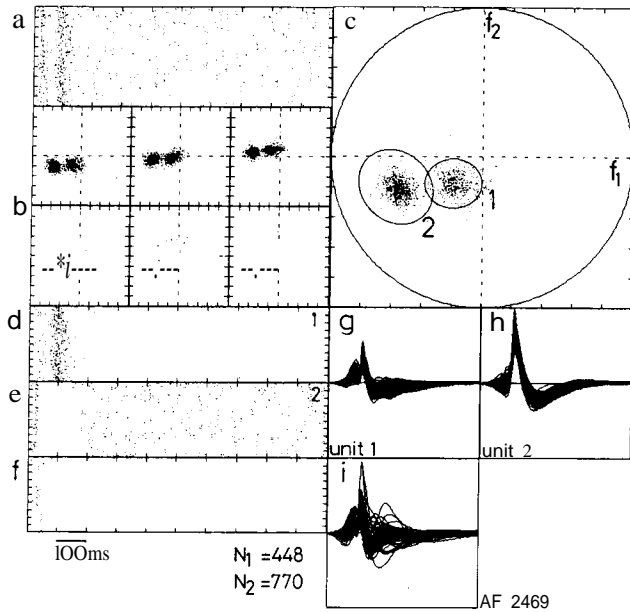


Fig. 5a-i. Separation and reconstruction of a double unit recording. In a the dot display is represented for the double-unit spike train with time base of 1 s. Tonepips lasting 48 ms were presented once per second. One observes a double band of stimulus locked spikes and spontaneous activity. b In six combinations of the four orthogonal templates the spike waveforms are represented, the combinations  $(f_1, f_2)$ ,  $(f_1, f_3)$  and  $(f_1, f_4)$  in the upper row, and  $(f_2, f_3)$ ,  $(f_2, f_4)$  and  $(f_3, f_4)$  in the lower row. It is observed that the three combinations including  $f_1$  provide a clear separation of clusters. c For the separation the  $f_1/f_2$  pair is selected and ellipses are drawn first to remove cluster 1 and then cluster 2. The dots that remain within the large circle are then considered unclassified. d-f shows the reconstructed single unit dot displays for both units and the unclassified spikes. g-i show the superimposed reconstructed waveforms for each spike in the recording, in i the unclassified spikes are collected

low pass filtered version of a i.e. the superimposed electrode noise generally is removed. In case the reconstruction of an average waveform (i.e. without noise) is attempted one obtains such good estimates that differences are hardly noticeable by visual inspection (Fig. 1).

#### 4 Correlation Functions for Spike Trains

Consider two spike trains  $z_1(t)$  and  $z_2(t)$  represented as  $Z_1(t) = \sum_{i=1}^{N_1} J(t-t_i)$  and  $Z_2(t) = \sum_{j=1}^{N_2} J(t-t'_j)$  and write the cross-correlation function as

$$R_{z_1 z_2}(\tau) = \frac{1}{T} \sum_{i=1}^{N_1} \sum_{j=1}^{N_2} \delta[\tau - (t'_j - t_i)]. \quad (1)$$

Using bin width  $\Delta$  the cross-coincidence function can be defined as

$$C_{z_1 z_2}(r, \Delta) = \frac{1}{\Delta} \int_{-1/2}^{1/2} da'' R_{z_1 z_2}(a'') \quad (2)$$

Table 1. Overview of the possible coincidence histograms

	$z_1$	$z_2$	$z_1'$	$z_2'$
$z_1$	$C_{11}$	$C_{12}$	$C_{11'}$	$C_{12'}$
$z_2$		$C_{22}$	$C_{21'}$	$C_{22'}$
$z_1'$			$C_{11'}$	$C_{12'}$
$z_2'$				$C_{22'}$

and the cross-coincidence histogram, on which the actual analysis is based as, (Aertsen et al., 1979).

$$C_n(L) = C_{z_1 z_2}(nL, \Delta) \quad \text{with } n = 0, \pm 1, \pm 2, \dots \quad (3)$$

This  $C_n(L)$  is an estimate of the probability of observing a spike in  $z_2(t)$  between  $t+(n-t)L$  and  $t+(n+t)L$  provided there was a spike in  $z_1(t)$  at  $t$ . In case of double unit recording (spike trains  $Z_1(t)$  and  $z_2(t)$ ) and presenting the same stimulus ensemble a second time (spike trains  $Z_1'(t)$  and  $z_2'(t)$ ) it is possible to compute 10 cross-coincidence histograms as arranged in the Table 1. For short we write  $C_{z_1 z_2}$  as  $C_{12}$  etc.

On the main diagonal we find the autocoincidence histograms for both units, which reveal the internal structure of the individual spike trains. Under stationary firing conditions  $C_{ii} = C_{i1'}$   $i = 1, 2$ . In practice we will use  $C_{ii} = \frac{C_{ii} + C_{i1'}}{2}$  as an estimator for the autocorrelation function of the spike trains. It is remarked that  $C_{k1}(r) = C_{1k}(-r)$ , therefore the matrix in Table 1 is symmetric, provided that the sign of  $r$  is adjusted.

Off the main diagonal we observe  $C_{12}$  and  $C_{12'}$  both representing the simultaneous cross-coincidence histogram between both units in the double unit recording. Again we will use  $C_{ij} = \frac{C_{ij} + C_{i'j'}}{2}$  as the estimator of the correlation in the firings of both units.

The non-simultaneous cross-coincidence histograms  $C_{12'}$  and  $C_{21'}$  are thought to represent only that correlation between unit 1 and unit 2 that is due to stimulus coupling (cf. Perkel et al., 1967).

Another cross-coincidence histogram is obtained by taking both spike trains for the same unit  $Z_i(t)$  and  $z_i(t)$  to obtain  $C_{11'}$  and  $C_{22'}$ . These cross-coincidence histograms represent the amount of stimulus locking of the units taken individually, hence it is a measure for the existence of a stimulus response relation (Aertsen et al., 1979).

Finally the presence of neural interaction may be revealed unambiguously by considering  $C_{12}$  for spontaneously active neurons in the absence of stimulation.

#### 5 Correction for Stimulus-Locked Activity

In case of acoustic stimulation a correction for effects of stimulus-influence on the spikes in the coincidence

histogram must be carried out. Depending on the nature of the relation between stimulus and neural interaction different correction procedures should apply.

First of all we consider the effect of the stimulus to be *additive*, i.e., adding spikes, and not to affect the neural interaction. This is in fact the model described by Perkel et al. (1967). We consider the spike train of the longer latency neuron to result from two types of spikes, those directly caused by the stimulus  $z_s(t)$  and those caused by activity of the shorter latency neuron or by spontaneous activity  $z(t)$ . The resulting spike trains are

$$Z_1(t) = Z_{1s}(t) + Z_{1n}(t) \quad \text{and} \quad Z_2(t) = Z_{2s}(t) + Z_{2n}(t).$$

Then the estimators of the simultaneous and non-simultaneous cross correlation functions between the two spike trains are

$$C_{12}(\tau) = E[Z_{1s}(t)Z_{2s}(t+\tau)] + E[Z_{1n}(t)Z_{2n}(t+\tau)]$$

and

$$C_{12}(\tau) = E[z_{1s}(t)z'_{2s}(t+\tau)]$$

since all other non-simultaneous correlations are flat. Under stationary conditions  $E[z_{1s}(t)Z_{2s}(t+\tau)] = E[z_{1s}(t)z'_{2s}(t+\tau)]$  so that

$$C_{12}(\tau) = E[z_{1s}(t)Z_{2n}(t+\tau)] + E[z_{1n}(t)Z_{2n}(t+\tau)] \quad (4)$$

can be used as an estimator for neural correlation. In case the first expected value is flat for all stimuli the neural correlation is stimulus independent. In general one expects even under an additive model some stimulus dependence, e.g. via unobserved neuronal inputs that contribute to  $z_{1n}(t)$  and  $z_{2n}(t)$ .

It must be remarked that the additive model (Perkel et al., 1967) is the only one currently used in stimulus correction procedures (e.g. Voigt and Young, 1980). However, Srinivasan and Bernard (1976) have shown that coincidence detecting neurons can produce an output that is based on a *multiplicative* action from two input neurons, provided that their spike trains are statistically independent. The criteria determining whether the action is additive or multiplicative are size of the excitatory post synaptic potential (EPSP) relative to threshold and the time constant of decay for the EPSP. EPSP values smaller than the threshold of firing and with a duration less than the average interspike interval of the individual spike trains cause the action to be multiplicative. Larger EPSP values or those with longer duration make the action additive. An alternative formulation from which this effect can be understood is that we consider a spike generator

with probability of firing,  $g$ , which depends sigmoidally on EPSP value  $u$  (Johannesma and van den Boogaard, in preparation).

$$g(z|u) = \frac{\exp(-3u)}{1 + \exp(-3u)} \quad (5)$$

Here  $u$  is simply considered to be the linear summation of contributions  $u_i$  caused by incoming spikes  $z_i$  possibly originating from different projecting neurons. Actually  $g(z|u)$  describes the well known S-shaped curve. For relatively small  $u$  values, i.e., in the purely exponential region of the curve and temporal overlap of  $u_1$  and  $u_2$  we have:

$$g(z|u_1, u_2) = \frac{\exp(-3(u_1 + u_2))}{1 + \exp(-3(u_1 + u_2))} \approx \frac{\exp(-3u_1)\exp(-3u_2)}{1 + \exp(-3u_1) + \exp(-3u_2)} \approx g(z|u_1) \cdot g(z|u_2) \quad (6)$$

If the  $u$  values are large enough to be in the linear, intermediate, part of the S-curve then after expansion of the exponential and long division:

$$g(z|u) \approx \frac{1}{2} + \frac{1}{4}\beta u \quad (7)$$

and in case  $u_1$  and  $u_2$  are non overlapping (low spike rates) averaging over time gives

$$g(z|u_1, u_2) \approx g(z|u_1) + g(z|u_2) \quad (8)$$

Thus simply on basis of the size  $u$  and duration of the EPSP the firing probability of the output neuron can be multiplicative or additive with respect to the input spike trains. In fact  $u = u(t)$  and additional conditions regarding the decay time constant may enter the description.

If we now consider that a multiplicative effect of the stimulus on spike train activity is present, e.g., by two input spike trains both depending on the stimulus and fulfilling the conditions for the EPSP but only one of these input trains is observed together with the output train. In such a case the degree of multiplicative action is strongly dependent on the type of stimulus. Stimuli such as continuous noise that cause the input spike trains to have a relatively large time jitter, i.e. have a broad existence function,  $C_{ii}(\tau)$ , (Aertsen et al., 1979), produce results that better fit a multiplicative model than stimuli that tend to lock the spikes to a considerable degree (e.g. tone pips) as suggested by the Srinivasan and Bernard (1979) model results.

Thus also multiplicative interaction effects may be stimulus dependent. In case they are not, the application of a correction procedure based on an additive model, however, erroneously will indicate a stimulus dependence of the neural correlation.

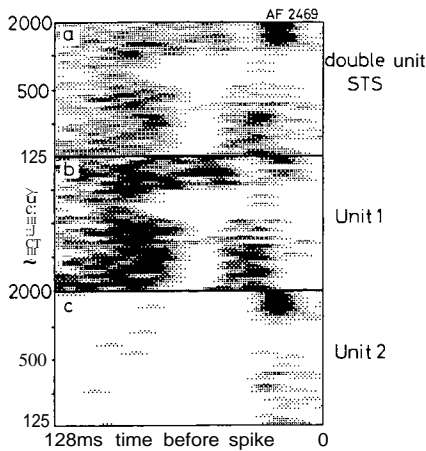


Fig. 6. Spectra-temporal sensitivities for the double unit recording and the separated single units. The average intensity of the tonal stimuli as a function of tone frequency and time before the spike is shown in grey code, darker areas represent larger intensities. One could consider this as the intensity distribution in frequency and time of stimuli best matched to the neural sensitivity. In this and all subsequent STS auto scaling of the intensity is used. It is observed that unit 2 is dominantly sensitive to tonepips having frequencies between 1 and 2 kHz (note log-frequency scale). Unit 1 is sensitive to nearly all frequencies albeit in a complicated manner

## Results

We will describe in some detail the findings in one double unit recording and one triple-unit recording with particular emphasis on the stimulus dependence of neural correlation.

### A Double Unit Recording

**A1** First of all the double unit dot display (Fig. 5a) shows the occurrence of the action potentials on a time base of 1 s. Tone pips, having a  $\gamma$ -function shaped envelope (Aertsen and Johannesma, 1980) with a duration of 48 ms and a frequency randomly selected out of 127 frequency values spaced equidistantly on a log scale over the range of 125-2000 Hz, are presented once per second. Thus the tonepip presentation is at the left hand side of the dot display. Four identical, random frequency, fixed peak amplitude (89 dB SPL) sequences are presented resulting in a total stimulus duration of 509 s (including some restart time). One observes spontaneous activity and in addition a double band of firings at approximately 30ms and 100ms after tonepip onset.

The set of six boxes below the dot display (Fig. 5b) represents the possible combinations of the four basis vectors used for the waveform analysis. Two different neurons are present, separation appears possible on  $(f1,f1)$ ,  $(f1,f3)$  and  $(f1,f4)$  indicating that 11 (the horizontal coordinate in the upper three projections) is the separating feature. The actual separation procedure was carried out on  $(f1,f2)$  as shown in Fig. 5c

and resulted in 448 spikes classified as unit 1 (being most near to the origin), 760 spikes as unit 2, while 76 spikes remained unclassified (about 5%). From the superposition of the waveforms one observes that the main difference is in the spike amplitude. The reconstructed single unit dot displays (Fig. 5d-f) show that unit 1 (Fig. 5d) responded mainly at about 100 ms after tone pip onset and also fired albeit somewhat less, around 30 ms; less or no spontaneous activity is observed. Unit 2 (Fig. 5e) clearly responded at a sharp 20ms latency, then was suppressed for nearly 150ms duration and thereafter resumed with spontaneous activity. The non-classified spikes (Fig. 5f) mostly had latencies in the 20-30 ms region.

**A2** In Fig. 6 the spectro-temporal sensitivities (STS) (Hermes et al., 1982) for the double unit combination (Fig. 6a) and for both units separately (Fig. 6b, c) are shown. A very complex picture emerges. We recall that darker regions in the picture correspond to higher values of the average stimulus intensity at that particular frequency that precedes the spike. The dark region in the upper right corner of the double unit STS corresponds to a short latency response in the dot display C~20ms) for tonepips with frequencies between 1 and 2 kHz. It is seen that this region is nearly completely due to the activity of unit 2, which besides that also shows short latency low frequency activity. In the dot display it was seen as the sharp line with ~ 20 ms latency, i.e., if the response comes 20 ms after tonepip onset then the average tonepip intensity will be large in the region preceding the spikes by 20 ms. Unit 2 then remains silent for nearly 150 ms and therefore no effect is seen in the 128 ms region preceding the spikes.

The complex part of the double unit STS is completely taken care of by unit 1. It appears that the 30 ms firings originate from responses to tonebursts with frequencies below 500 Hz, the major activity (at 100 ms latency) arises from the whole frequency range covered.

We may interpret the STS of unit 1 as indicating activity over a large latency range from basilar papilla units (1-2 kHz) and repeated activity from amphibian papilla input ( $< 500$  Hz). The STS of unit 2 indicates dominantly short latency input from basilar papilla units.

**A3** One may wonder if unit 2, the short latency one, provides an excitatory input for unit 1 especially in the basilar papilla range. On the other hand one may have the impression that unit 1 suppresses activity in unit 2. A combination of both mechanisms is also possible. To test these hypotheses a correlation analysis has been performed on the spike trains from unit 1 and 2. Figure 7 shows the correlation histograms as discussed



in the method section, the upper row of boxes (Fig. 7a) displays the auto-coincidence functions pointing at the repeated activity of unit 1 (average interval  $\sim 60$  ms) and the spontaneous activity of unit 2. The second row (Fig. 7b) shows the amount of stimulus lock of both units: the rather broad peak found for unit 1 expresses the relatively poor synchronization of the firings with toneburst onset. For unit 2 the spontaneous activity obscures the stimulus lock that could be seen in the dot displays. The third row of boxes (Fig. 7c) shows the simultaneous and non-simultaneous cross-coincidence functions: the first  $C_{12}$  comprises neural interaction as well as various effects of stimulus coupling, the second  $C'_{12}$  can only contain stimulus coupling. Finally the last functions  $C_{12}-C'_{12}$  should indicate neural correlation effects, if any. It can be seen that the effects presumed on studying the dot displays and spectrotemporal receptive fields cannot be substantiated by the correlation analysis.

A4 The double unit preparation was also stimulated with continuous pseudorandom noise, both 5 kHz and 1.5 kHz (-3 dB) low pass noise was used. The separated single unit dot displays to the 1.5 kHz lowpass noise are shown in Fig. 8. The length of one pseudorandom noise sequence was 34.9525 s and one half of it was used as the time base length in the dot displays. The total stimulus duration is 560 s. For both units the transient onset in activity is observed, stationarity of the firing pattern is observed after 2 sequences (i.e. about 70 s). Unit 2 shows some very clear vertical patterns indicating that this unit fired nearly always and at nearly the same time for these parts of the noise stimulus. In unit 1 this is harder to detect. If we recall, however, that unit 1 did not show spontaneous activity we must nevertheless conclude that it was activated by the noise. Calculating STS's for this noise stimulus (Hermes et al., 1981) did not reveal any result for unit 1, while for unit 2 diffuse sensitivity could be demonstrated between 150 and 750 Hz and extending from 78.28 ms to about 10 ms before the spike (Fig. 9). No activity was observed in the basilar papilla range in sharp contrast to the tonal analysis. Comparing with Fig. 6 shows that the weak activity of unit 2 in the low frequency region for tonal stimuli is the only region that is also responding to continuous noise.

A5 The correlation analysis (Fig. 10) shows striking differences as compared to the results for tonal stimuli (Fig. 7). First of all the repeated firing character of unit 1 is no longer observed while it now shows up in unit 2 (Fig. 10a) as close inspection of the dot display (Fig. 8b) also reveals. The stimulus coupling (Fig. 10b) is now especially pronounced in unit 2 although some impression can be seen in unit 1. Considering that during tonal stimulation unit 2 had an average firing

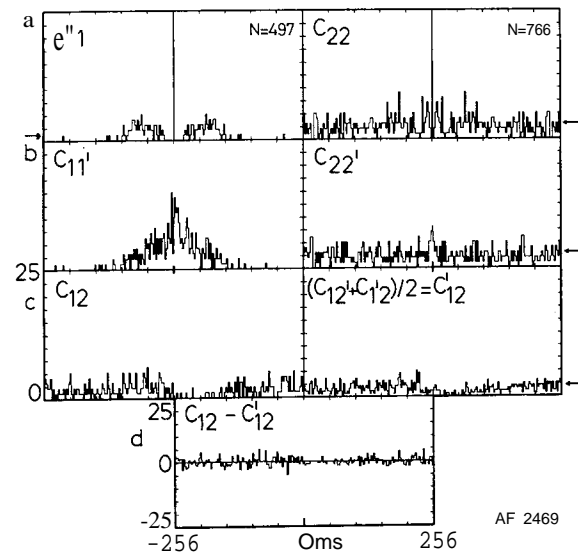


Fig. 7a-d. Survey of coincidence histograms for double unit recordings. Used are spike trains evoked by presenting 48 ms tonepips with randomly selected frequency once per second. Two units (1 and 2) are recorded simultaneously and a repeated recording is also obtained (1' and 2'). a shows the autocoincidence functions of units 1 and 2; one observes signs of repeated firing with intervals of about 50-60 ms in  $C_{11}$ . b shows so called existence histograms: a unit's spike train is correlated with its repeat, this indicates the amount of stimulus lock. One observes that the spontaneous activity of unit 2 nearly destroys any sign of stimulus coupling. c the crosscoincidence between units 1 and 2 is given for simultaneous and non-simultaneous recorded spike trains. The difference in d should indicate neural correlation, if any. The arrows indicate the expected values for spike trains with Poisson statistics

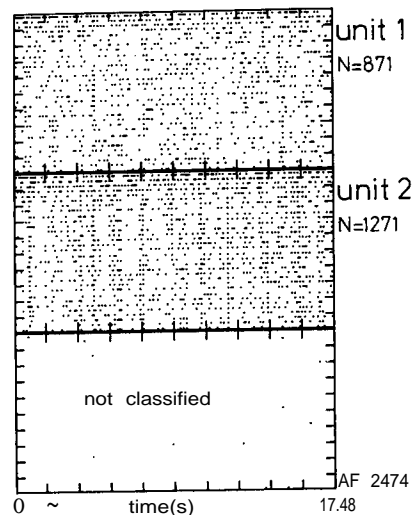


Fig. 8. Dot displays for separated single units to pseudorandom noise. Used is a noise sequence length of about 35 s, as time base for the dot display half this value is used. One observes, especially for unit 2, a vertical line pattern indicating that the unit fired with good stimulus coupling to specific parts of the noise. A certain transient onset effect on the number of firings is noted

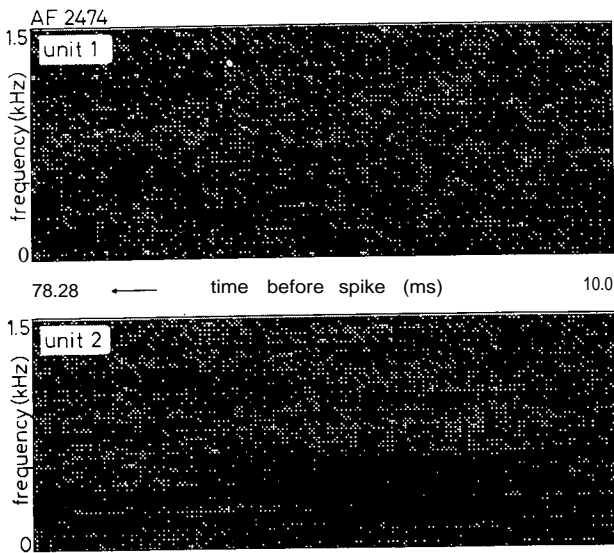


Fig. 9. The spectro-temporal sensitivities of the double unit pair to noise. These Figures indicate using a linear frequency scale the average noise intensity that precedes spikes. Black indicates more than average intensity, white less than average intensity. One observes for unit 2 that in the low frequency range (100-500 Hz) there is a broad excitation region. It must be noted that although unit 2 appeared to be sensitive to 1-2 kHz tonepips dominantly (cf. Fig. 6) there was no response to continuous 5 kHz bandwidth noise

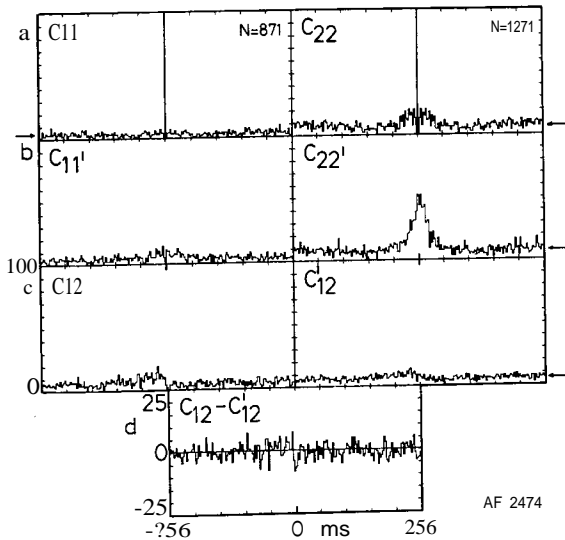


Fig. 10. Coincidence histogram analysis of the double unit for continuous noise stimulation. In part b one observes that there is a clear stimulus coupling for unit 2. The arrows indicate the expected values in case the spike trains showed a Poisson character. They are the same for  $C_{11}$  and  $C_{11}'$ , as well as for  $C_{12}$  and  $C_{12}'$ . Further explanation in Fig. 7

rate of  $1.5 s^{-1}$  and during noise stimulation  $2.5 s^{-1}$  we conclude that the noise not only rearranged the spontaneous activity but also added about 1 spike per second. The simultaneous and non-simultaneous crosscoincidence functions (third row) look slightly

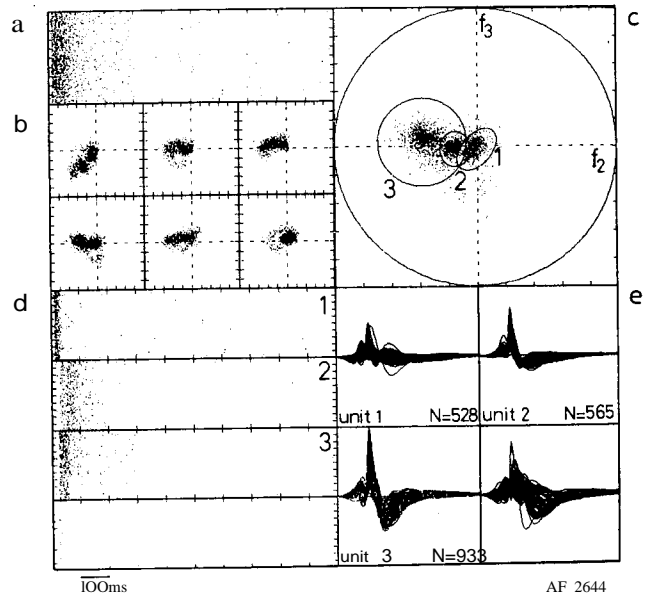


Fig. 11a-e. Separation and reconstruction for a triple unit recording. a shows the triple-unit dot display, b shows the projections of the individual waveforms on the templates c shows the selected  $f_2, f_3$  pair for the separation procedure. First the spikes belonging to unit 1 are removed, then for unit 2 and finally for unit 3, the remaining spikes being left unclassified. In part d the single unit dot displays are reconstructed and in part e the spike waveforms. Stimulation was with 48 ms tonepips presented once per second

different, but the subtraction does not clearly reveal this. We are therefore forced to conclude that neural correlation between these two units could not be demonstrated.

### B Triple Unit Recording

*Bi* The stimulus dependence of the STS's and the various correlation functions will be elaborated upon by using the results of a triple unit recording. Figure 11 shows the overall findings for stimulation with 48 ms duration tonepips presented once per second. The general format is the same as in Fig. 5. The triple unit dot display (Fig. 11a) reveals stimulus locked activity from about 10-80ms following the presentation of the tonepips followed by spontaneous activity. Separation on basis of the projections appeared to be possible on  $(f_1, f_3)$  as seen in Fig. 11c. Recall that the separation procedure is sequential, first the unit most close to the origin is selected and all the spikes within the ellipse indicated by 1 are removed from the data file. Subsequently the small cluster is removed and then the largest one indicated by 3. The resulting spike waveforms differ in waveform as well as amplitude. The reconstructed single unit dot-displays (Fig. 11d) show for unit 1 (most close to the origin) that the responses fell in a short latency activity band mostly followed by some spontaneous activity. Unit 2 fired in a fuzzy

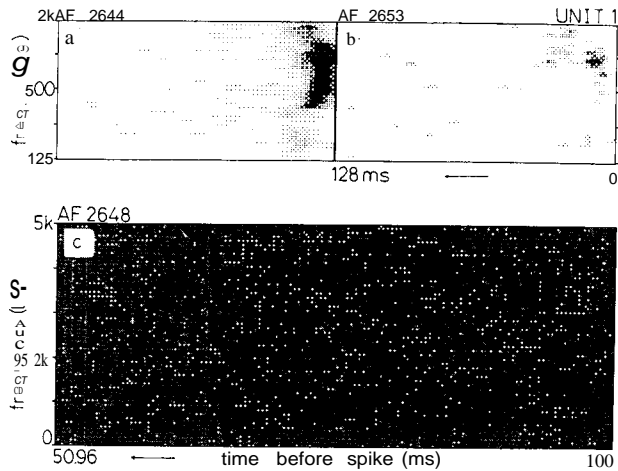


Fig. 12a-. Spectro-temporal sensitivities (STS) for unit 1 for stimulation with 48 ms tonepips presented once per second a; 16 ms tonepips presented once per 128 ms b, and continuous 5 kHz bandwidth pseudorandom noise c. In all cases the time before the spike is indicated. For the tone pip stimuli the time base lasts 128 ms and frequency is on log scale. For the noise stimulation the time base runs from 50.96ms to 10.0ms before the spike and frequency is on linear scale. No STS can be observed for noise. The unit appears to be mostly sensitive to tone frequencies around 1 kHz

broad latency range after the cessation of firing of unit 1. Unit 3 finally responded with a latency intermediate between unit 1 and 2. About 4% of the spikes remained unclassified.

**B2** Besides the stimulus sequence just discussed we presented to these units also continuous pseudorandom noise low-passed at 5 kHz (-3 dB) and a sequence of short duration (16 ms) y-tones presented each 128 ms. We will first discuss for each of the 3 units the STS's as determined with these three stimulus ensembles.

**B2a Unit 1** (Fig. 12) responded (528 spikes) with a 15 ms latency to 48 ms tonebursts presented once per second if the frequencies were around 750 Hz and 1250 Hz. This unit therefore seems to receive input from the basilar papilla as well as from the amphibian papilla (Fig. 12a). For stimulation with 16ms y-tones presented each 128 ms this unit fired only 86 times and the STS only showed short latency activity for the 1250 Hz region. This is compatible with a functional threshold increase, probably due to adaptation effects. For stimulation with noise the unit was slightly more active especially during the first noise sequence (lasting 10.48575 s) a total number of spikes obtained was 198. The STS (Fig. 12c) did not reveal any significant spectro-temporal sensitivity.

**B2b Unit 2** (Fig. 13) responded with 565 spikes to 48 ms y-tones presented once per second. The STS is broad both in the frequency domain (250 Hz-2000 Hz)

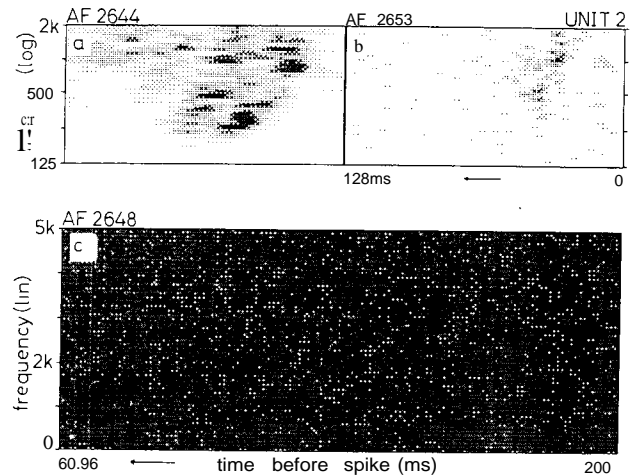


Fig. 13a-. Spectro-temporal sensitivities (STS) for unit 2 for stimulation with both tonal stimulus ensembles and noise. In part a a broad STS is found to stimulation with one 48 ms tonepip per second. In part b one observes that with faster repetition of shorter tonepips, (16 ms, once per 128 ms) the unit has no clear STS. No STS can be found for noise stimulation either

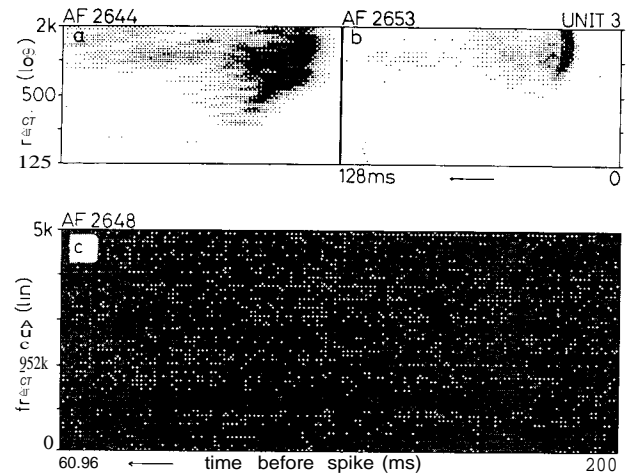


Fig. 14a-. Spectro-temporal sensitivities (STS) for unit 3 to stimulation with tonal stimulus ensembles and noise. Clear STS are observed for all three stimulus ensembles, maximum sensitivity is around 1250 Hz for noise c, between 1 and 2 kHz for 16 ms tonepips presented each 128 ms b and between 500 Hz and 1 kHz as well as between 1 and 2 kHz for the 48 ms tonepips presented once per second a

and in the temporal domain (128 - 0 ms before the spikes). The main activity is produced by the 300 Hz and 1 kHz regions and this unit therefore also receives input from the basilar papilla as well as the amphibian papilla. In response to 16 ms y-tones presented at 128 ms intervals the number of spikes was 203 and the STS (Fig. 13b) can again be considered as if produced in a situation with a functionally elevated threshold. Noise was not very effective in producing only 182 spikes, the STS did not reveal any specific sensitivity.

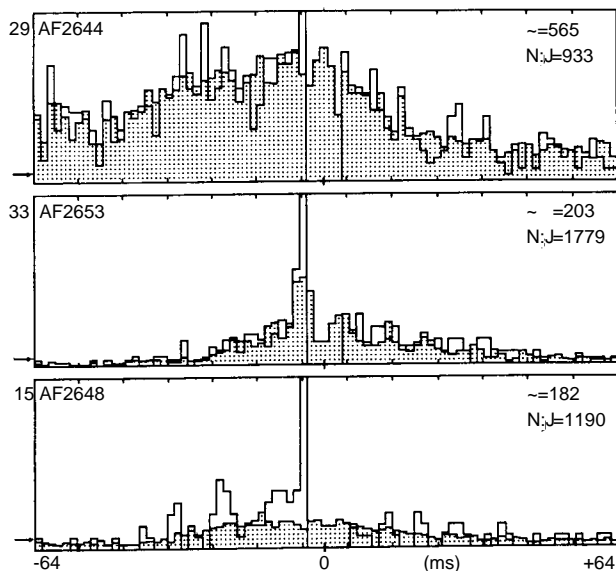


Fig. 15. Simultaneous and non-simultaneous cross coincidence histograms for units 2 and 3 under tonal and noise stimulation. The non-simultaneous cross coincidence histograms are shaded. The difference between both histograms is a measure for the strength of the neural correlation, it is observed that this difference is negligible for stimulation with 48 ms tonepips presented once per second (upper); is confined to a few bins in case stimulation was done with 16 ms tonepips presented once per 128 ms (middle); and is quite clear for noise stimulation (lower)

Table 2. Coincidences for double unit spike trains

	Present	Doubtful	Absent	Total
Synchrony	22	5	4	31
Correlation	4	4	14	22
Stimulus dependence	3	0	1	4
Interaction	1	2	3	6

*B2c Unit 3* (Fig. 14) responded with 933 spikes to 48 ms y-tones presented once per second. The STS shows a relatively short latency broad tuning with activity both from the amphibian and basilar papilla. As in unit 2 the high-frequency activity suggests repeated firing. For 16 ms y-tones (Fig. 14b) the unit responded with 779 spikes mostly having a latency of 20 ms. The activity was nearly exclusively produced by the 1-2kHz frequency region. Noise appeared to be an effective stimulus also in evoking 1190 spikes. The STS showed a relatively small spectral width around 1250 Hz but a very pronounced temporal extension ranging from 60 ms - 30 ms prior to the spikes. This spectral and latency range is comparable to the result obtained with the 16ms y-tones.

*B3* All cross-coincidence functions between unit 1 and unit 2 appeared to be the same for the simultaneous and non-simultaneous situation. Therefore all cor-

relation between the spike trains of these two units could be accounted for by stimulus lock. Basically the same was found between units 1 and 3.

A different situation was found for units 2 and 3. We will discuss here only the simultaneous and non-simultaneous cross-coincidence functions and their difference

a. 48 ms y-tones presented once per second. In this situation (Fig. 15a) both cross-coincidence functions are nearly identical, the difference is nearly zero.

b. 16 ms y-tones presented once each 128 ms. In this case (Fig. 15b) we observe a difference in two bins prior to the dead-time region

c. noise stimulation, also here (Fig. 15c) the difference between the simultaneous and non-simultaneous cross-coincidence function is largest in the two bins preceding the dead-time but is also different from zero in the five bins preceding this one.

We might therefore conclude that the neural correlation strength depends on the type of stimulus used.

We analysed the occurrence of stimulus dependent neural correlation in a population of 11 grassfrogs from which 51 single unit recordings, 16 double unit recordings, three triple unit recordings and one quadruple unit recording were obtained. This resulted in a total number of 96 single unit records and 31 double unit combinations. For six double units we obtained sufficiently long spontaneous activity records to analyse the presence of neural interaction. In Table 2 the occurrence of neural synchrony, neural correlation and stimulus dependence of the neural correlation is indicated as well as the conclusions from the spontaneous activity records.

One observes that in 22 double unit combinations a clear neural synchrony was present between the firings of the simultaneously recorded single units. In only four out of these 22 a clear neural correlation remained after correction for stimulus influences under the assumption of an additive model. Three out of these four pairs showed a clear stimulus dependence of the neural correlation. In only one out of six double unit recordings under non-stimulus conditions could we demonstrate a clear neural interaction.

## Discussion

### *The Separation Procedure*

When considering Figs. 5 and 11 one may wonder whether the separation procedure has unambiguously resulted in the spike trains of the contributing units. From Fig. 5c we estimate that only up to ten spikes in the overlap region of the separation ellipses out of a total of 1294 may have been misclassified, while a larger number (76) is left unclassified. Effects of mis-

classification will be pronounced in the computation of the coincidence histograms,  $C_{12}$  and  $C_{12}'$ . The effects of not classifying may also affect the spectro-temporal sensitivities (e.g. Fig. 6).

Considering the smallness of the number of optionally misclassified spikes in the double unit recording and furthermore considering the differences in latency between unit 1 and 2 we assume that the low frequency short latency part of the STS for unit 2 (Fig. 6) is real and not due to erroneously classified spikes from unit 1. The same holds vice versa for the short latency, high frequency part of the STS for unit 1.

The situation exemplified in Fig. 11 may look more severe while the spike waveform reconstructions (Fig. 11e) may suggest a few actual misclassifications. However, the response properties of unit 2 and 3 differ completely with respect to their STS for noise (Figs. 13c and 14c), while those for units 1 and 2 (Figs. 12a, band 13a, b) are clearly separated according to latency. Since unit 1 has a smaller amplitude (on average) than unit 2 and also a shorter latency than unit 2, the possibility that repetitive firing of one unit which may cause a decrease in spike amplitude for the second and third firings caused us to separate spikes from one unit into two spiketrains can safely be ruled out. Furthermore neural units from the torus semi-circularis of the grassfrog never show interspike intervals shorter than 5-6 ms (at 15 DC). Misclassification in such case would produce peaks in the coincidence histogram  $C_{12}$  at  $r$ -values around 5-6 ms, in any case longer than found for these particular double unit combinations (cf. Fig. 15a-c). In this latter example the unclassified spikes (about 4% of the total number of 2105) mostly had large amplitudes and could result from a superposition of spike waveforms from unit 1 and 2, the presence of a fourth neural unit can, however, not be completely excluded.

Based on the combined separation-reconstruction procedure and on the information from the STS of the neural units, a relatively safe and reliable procedure for studying the correlation between spike trains separated from a multi unit record is obtained.

#### *The Stimulus-Correction Procedure*

In the methods section we argued against the use of arbitrary stimulus correction procedures when the underlying neural network model is unknown. Since this lack of information is nearly always interfering with the selection of the procedure, we applied the most simple correction model. It is a purely additive model in which a separation is understood between direct stimulus spikes, i.e., those spikes that are contributing to pronounced effects in the coincidence histograms  $C_{11}$ , and  $C_{12}$ , and other spikes. These other

spikes might indirectly depend on the stimulus i.e. mediated through unobserved interneurons, general increase of firing probability etc. In this case the  $E[Z(t)Z(t+r)]$  in (4) may not be flat and stimulus dependent correlations can be found. In case the  $n$ -spikes are not due to any stimulus effect  $E[Z(t)Z(t+r)]$  is flat. The correction procedure in that case may reveal a pure neural interaction effect  $E[\ln(t)Z(t+r)]$  provided that the model hypothesis is correct. In general the model is unknown and one therefore can only speak about neural correlation instead of neural interaction. In case the neural correlation is stimulus dependent this does not yet imply that the connectivity between the neural units is modified by the stimulus. The effect of the stimulus may simply be in the activation or suppression of other neural units within the same neural net. The influence of these unobserved neurons might be revealed in cases where more units are recorded simultaneously by comparison of paircorrelations, triple correlations etc.

In case that application of the correction procedure results in a neural correlation which is close to zero (cf. Figs. 7 and 10) the possibility of a functional connection between the units is not ruled out: uncorrelated does not imply independent. Such situations might arise when the firings of both units are strongly locked to the stimulus and therefore  $E[Z(t)Z(t+r)]$  is about equal to  $E[Z(t)Z(t+r)]$  and much larger than any of the other terms. The difference between  $C_{12}$  and  $C_{12}'$  will then be quite close to the statistical fluctuations.

#### *The Forward and Backward Approaches to Stimulus-Response Relationships*

In our experimental approach (e.g. Figs. 5 and 6) we use both dot displays as well as the spectro-temporal sensitivity as measures for stimulus-response relationships. The first method monitors the neuronal activity in order to obtain estimates of firing probability as a function of e.g. stimulus frequency. Averages over subsets of stimuli may lead to PSTH's, this is the approach that is used in most auditory research.

The backward or reverse approach centers around the concept of the pre-event stimulus ensemble (Johannesma, 1972; Aertsen et al., 1980; Hermes et al., 1981) which is a subset of the stimulus ensemble that precedes action potentials. By averaging the pre-event stimulus ensemble, or in the present case the intensity values thereof, we obtain spectro-temporal sensitivities. These form a representation of the average stimulus intensity as a function of both frequency and time before an action potential. The STS may also be viewed as the sonogram of the sound which best matches the filter properties of the neural unit.

The combination of dot displays and STS offers a firm basis for the characterisation of neural units under the particular choice of the stimulus ensemble.

#### *Stimulus Dependence of Neural Correlation and Spectro-Temporal Sensitivity*

In previous work it was demonstrated that for neurons in the torus semicircularis of the grassfrog the spectro-temporal sensitivity in general is not invariant for the stimulus ensemble used (Aertsen and Johannesma, 1981a and b). It proved to be impossible to obtain the same STS for a tonal stimulus ensemble and an ensemble composed of natural sounds, even after the application of corrections for spectral and temporal differences between the stimuli. This holds also in comparison to spectro-temporal sensitivities determined for noise stimuli, as shown by Johannesma and Eggermont (1983). In general the STS for noise, tonal stimuli and ensembles consisting of species-specific vocalisations are different and cannot be brought in register by normalisation procedures based on the Wiener-Volterra formalism for the analysis of non-linear systems (Aertsen and Johannesma, 1981a).

The STS of a neuron generally depends in a non-linear way on the STS's of the projecting neurons. Some of these neurons may provide excitatory input, other inhibitory input. Part of the neural spike trains may cause the neuron to act in a multiplicative way, other spike trains result in an additive action depending on EPSP size and duration as well as firing rates. The resulting STS depends to a large extent on the way the neural net is influenced by the stimulus. Phasic neurons will behave quite differently for a continuous noise stimulus than for the repetitive presentation of short tonebursts and their effects on other neurons in the net change therewith.

Stimulus dependent neural correlation may therefore be strongly related to the stimulus dependence of the STS found in the majority of neurons from the torus semicircularis. This strongly suggests also that a stimulus invariant STS, referred to as spectro-temporal receptive field (STRF, Aertsen and Johannesma, 1981a), does not exist on the single neuron level, except at the level of the auditory nerve and simple units in higher auditory nuclei.

It seems much more plausible to determine multi-unit spectro-temporal sensitivities but with certain conditions imposed on the spikes that are taken into account. These conditions might well be derived from the results of the neural correlation studies. As such these conditional STS's bear some relationship to the logical response planes developed by Stevens and Gerstein (1976). Conditional STS's for different numbers of units that are synchronized or correlated could

be vehicles to understand the feature extraction mechanisms of the brain and might also offer a way to approach the properties of neural assemblies (palm, 1982; Shaw et al., 1982) provided a sufficiently large number of neurons can be recorded from simultaneously.

*Acknowledgements.* This investigation was supported by the Netherlands Organization for the Advancement of Pure Research (ZWO). Peter Johannesma was instrumental in the development of many ideas. Jan Bruijns and Wim van Deelen supported all computer procedures. Hans Krijt and his electronic workshop realised the spike waveform analyzer. Koos Braks prepared the grassfrogs for each experiment. Marianne Nieuwenhuizen prepared the manuscript.

#### References

- Abeles, M., Goldstein, M.H., Jr.: Multispike train analysis. Proc. IEEE 65, 762-773 (1977)
- Aertsen, AM.HJ., Johannesma, P.I.M.: Spectro temporal receptive fields of auditory neurons in the grassfrog. I. Characterization of tonal and natural stimuli. BioI. Cybern. 38, 223-234 (1980)
- Aertsen, AM.H.J., Johannesma, P.I.M.: The spectro-temporal receptive field. A functional characterization of auditory neurons. BioI. Cybern. 42, 133-143 (1981a)
- Aertsen, AM.HJ., Johannesma, P.I.M.: A comparison of the spectro-temporal sensitivity of auditory neurons to tonal and natural stimuli. BioI. Cybern. 42, 145-156 (1981b)
- Aertsen, AM.HJ., Johannesma, P.I.M., Hermes, DJ.: Spectro-temporal receptive fields of auditory neurons in the grassfrog. II. Analysis of the stimulus-event relation for tonal stimuli. BioI. Cybern. 38, 235-248 (1980)
- Aertsen, A.M.HJ., Smolders, J.W.T., Johannesma, P.I.M.: Neural representation of the acoustic biotope: on the existence of stimulus-event relations for sensory neurons. BioI. Cybern. 32, 175-185 (1979)
- Brzoska, J., Walkowiak, W., Schneider, H.: Acoustic communication in the Grass Frog (*R. temporaria*): calls, auditory thresholds and behavioral responses. J. Compo Physiol. 118, 173-186 (1977)
- Creutzfeldt, O., Hellweg, F.-C., Schreiner, Chr.: Thalamocortical transformation of responses to complex auditory stimuli. Exp. Brain Res. 39, 87-104 (1980)
- Dickson, J.W., Gerstein, G.L.: Interaction between neurons in auditory cortex of the cat. J. Neurophysiol. 37, 1239-1261 (1974)
- Dinning, GJ., Sanderson, AC.: Real-time classification of multi unit neural signals using reduced feature sets. IEEE BME-28, 804-811 (1981)
- Eggermont, JJ., Aertsen, AM.HJ., Hermes, DJ., Johannesma, P.I.M.: Spectro temporal characterization of auditory neurons: redundant or necessary. Hearing Res. 5, 109-121 (1981a)
- Eggermont, U., Hermes, DJ., Aertsen, A.M.HJ., Johannesma, P.I.M.: Response properties and spike waveforms of single units in the torus semicircularis of the grassfrog (*Rana temporaria*) as related to recording site. In: Neuronal mechanisms in hearing, Syka, J., Aitkin, L. (eds.) New York: Plenum Press 1981b, pp. 341-346
- Ewert, J.-P., Burghagen, H., Albrecht, L., Kepper, J.: Effects of background structure on the discrimination of configurational moving prey dummies by Toads *Bufo bufo* (L.). J. Compo Physiol. 147, 179-187 (1982)
- Fukunaga, K.: Introduction to statistical pattern recognition. New York: Academic Press 1972
- Gerstein, G.L.: Functional association of neurons: detection and interpretation. Neurosci. Second study program 648-661 (1970)

- Getchell, Th. V.: Analysis of unitary spikes recorded extracellularly from frog olfactory receptor cells and axons. *J. Physiol.* **234**, 533-545 (1973)
- Glaser, E.M.: Separation of neuronal activity by waveform analysis. *Adv. Biomed. Eng.* **1,77-136** (1971)
- Grover, F.S., Buchwald, J.S.: Correlation of cell size with amplitude of background fast activity in specific brain nuclei. *J. Neurophysiol.* **33**, 160-171 (1970)
- Heierli, P., Ribaupierre F. de, Toros, A, Ribaupierre, Y. de: Functional organization of the medial geniculate body studied by simultaneous recordings of single unit pairs. In: *Neuronal mechanisms of hearing*, Syka, J., Aitkin, L. (eds.). New York: Plenum Press 1981, pp. 183-186
- Hermes, D.J., Aertsen, AM.H.J., Johannesma, P.I.M., Eggermont, J.J.: Spectro temporal characteristics of single units in the auditory midbrain of the lightly anaesthetised grassfrog (*Rana temporaria* L.) investigated with noise stimuli. *Hearing Res.* **5**, 145-179 (1981)
- Hermes, D.I., Eggermont, J.I., Aertsen, AM.H.I., Johannesma, P.I.M.: Spectro temporal characteristics of single units in the auditory midbrain of the lightly anaesthetised grassfrog (*Rana temporaria* L.) investigated with tonal stimuli. *Hearing Res.* **6**, 103-126 (1982)
- d'Hollander, E., Orban, G.A.: Spike recognition and on-line classification by unsupervised learning system. *IEEE Trans. BME* **26**, 279-284 (1979)
- Johannesma, P.I.M.: The pre-response stimulus ensemble of neurons in the cochlear nucleus. In: *Proceedings of the IPO Symposium on Hearing Theory*, Cardozo, B.L. (ed.). Eindhoven 1972, pp. 58-69
- Johannesma, P., Eggermont, J.: Receptive fields of auditory neurons in the midbrain of the frog as functional elements of acoustic communication. In: *Advances in Vertebrate Neuroethology*, Ewert, J.-P., Capranica, R.R., Ingle, D.J. (eds.). New York: Plenum Publishing Corporation (in press)
- Johnson, D.H., Kiang, N.Y.S.: Analysis of discharges recorded simultaneously from pairs of auditory nerve fibers. *Biophys. J.* **16**, 719-734 (1976)
- Kiang, N.Y.S., Watanabe, T., Thomas, E.C., Clark, L.F.: Discharge patterns of single fibers in the cats auditory nerve. Cambridge: MIT Press 1965
- Lombard, R.E., Fay, R.R., Werner, Y.L.: Underwater hearing in the frog, *Rana catesbeiana*. *J. Exp. Biol.* **91**, 57-71 (1981)
- Osen, K.K.: Cytoarchitecture of the cochlear nuclei in the cat. *J. Comp. Neurol.* **136**, 453-482 (1969)
- Palm, G.: Neural assemblies. An alternative approach to artificial intelligence. In: *Studies in Brain Function*, Vol. 7, Berlin, Heidelberg, New York: Springer 1982, pp. 1-244
- Paton, JA, Kelley, D.B., Sejnowski, T.I., Yodowski, M.L.: Mapping the auditory central nervous system of *Xenopus laevis* with 2-deoxyglucose autoradiography. *Brain Res.* **249**, 15-22 (1982)
- Perkel, D.H., Gerstein, G.L., Moore, G.P.: Neuronal spike trains and stochastic point processes. **II**. Simultaneous spike trains. *Biophys. J.* **7**, 419-440 (1967)
- Pfeiffer, R.R.: Anteroventral cochlear nucleus: waveforms of extracellularly recorded spike potentials. *Science* **154**, 667-668 (1966)
- Robertson, D.: Possible relation between structure and spike shapes of neurones in guinea pig cochlear ganglion. *Brain Res.* **109**, 487-496 (1976)
- Shaw, G.L., Harth, E., Scheibel, AB.: Cooperativity in Brain Function: Assemblies of Approximately 30 Neurons. *Exp. Neurol.* **77**, 324-358 (1982)
- Srinivasan, M.V., Bernhard, G.D.: A proposed mechanism for multiplication of neural signals. *Biol. Cybern.* **21**, 227-236 (1976)
- Stevens, J.K., Gerstein, G.L.: Interactions between Cat lateral geniculate neurons. *J. Neurophysiol.* **39**, 239-256 (1976)
- Suga, N.: Feature extraction in the auditory system of bats. In: *Basic Mechanisms in Hearing*, Meller, A (ed.). New York: Academic Press 1973, pp. 675-742
- Syka, J., Radionova, E.A, Popelar, J.: Discharge characteristics of neuronal pairs in the rabbit Inferior Colliculus. *Exp. Brain Res.* **44,11-18** (1981)
- Vibert, J.F., Costa, J.: Spike separation in multi unit records: A multivariate analysis of spike descriptive parameters. *EEG Clin. Neurophysiol.* **47**, 172-182 (1979)
- Voigt, H.F., Young, E.D.: Evidence of inhibitory interactions between neurons in dorsal cochlear nucleus. *J. Neurophysiol.* **44**, 76-96 (1980)
- Witpaard, J., Keurs, H.E.D.J. ter: A reclassification of retinal ganglion cells in the frog, based upon tectal endings and response properties. *Vision Res.* **15**, 1333-1338 (1975)

Received: December 28, 1982

J. J. Eggermont  
 Department of Medical Physics and Biophysics  
 University of Nijmegen  
 Geert Grooteplein Noord 21  
 NL-6525 EZ Nijmegen  
 The Netherlands